

Shape memory crosslinked polyurethanes containing thermoreversible Diels-Alder couplings

Csilla Lakatos,¹ Katalin Czifrák,¹ József Karger-Kocsis,² Lajos Daróczi,³ Miklós Zsuga,¹ Sándor Kéki¹

¹Department of Applied Chemistry, University of Debrecen, Egyetem tér 1, H-4032, Debrecen, Hungary

²Department of Polymer Engineering, Budapest University of Technology and Economics, Műegyetem rkp. 3, H-1111, Budapest, Hungary

³Department of Solid State Physics, University of Debrecen, Bem tér 18/b, H-4026, Debrecen, Hungary

Correspondence to: S. Kéki (E-mail: keki.sandor@science.unideb.hu)

ABSTRACT: Crosslinked polyurethanes (PUs) containing irreversible (allophanate) and reversible Diels-Alder chemical bonds were synthesized using various diisocyanates (methylene diphenyl diisocyanate MDI, 1,6-hexamethylenediisocyanate HDI) and poly(ϵ -caprolactone) (PCL) with different molecular weights ($M_n = 10$ kg/mol, 25 kg/mol, 50 kg/mol) as diol component. The melting/crystallization of PCL and the reversible DA bonds acted as temperature-activated switches for shape memory performances, while allophanate network provided the permanent crosslinks for these PUs. The reversible DA bonds were obtained by the reaction of diisocyanate-ended prepolymers with furfurylamine (FA) followed by the addition of bismaleimide (BMI). The permanent crosslinks between the linear chains containing DA bonds were achieved using additional amounts of diisocyanates (MDI or HDI). The above reaction path was supported by infrared spectroscopic results and swelling experiments. Tensile mechanical and shape memory properties in tension of the PUs were determined and discussed as a function of composition and crosslink densities deduced from swelling and dynamic mechanical analysis. © 2016 Wiley Periodicals, Inc. *J. Appl. Polym. Sci.* **2016**, *133*, 44145.

KEYWORDS: copolymers; crosslinking; morphology; polyurethanes; structure-property relations

Received 25 March 2016; accepted 26 June 2016

DOI: 10.1002/app.44145

INTRODUCTION

Shape memory polymers (SMPs) is a special class of polymers that are able to change their shapes (sizes) in a controlled manner upon the effect of external stimuli such as light, moisture, pH, heat, etc.^{1,2} Among the SMPs those with thermoresponsive properties became under spot of interest for possible applications in different fields. Thermoresponsive SMPs consist of amorphous or semicrystalline domains which may act as switches for temporary shaping, while physical or chemical crosslinks (also on supramolecular levels) serve as netpoints for the permanent shape.^{3,4} Incorporation of reversible chemical bonds into the polymer networks is a further tool for the alteration of crosslink density, and hence the mechanical properties, as a function of the temperature. The thermal reversibility of chemical bonds plays a significant role in the recent development of SMPs.^{5,6}

Such specific linkages can be formed by making use of various methods of the click chemistry, and especially by triggering the

Diels-Alder (DA) reaction between a dienophile and a diene.⁷ A further beauty of the DA reaction is that it can be performed in aqueous media, solutions, and melts, as well. DA adducts can be repeatedly generated after retro DA reactions liberating the initial functional groups. This feature has been used to demonstrate the feasibility of intrinsic self-healing.⁸ This pioneering work triggered vivid interest for adapting DA reactions for self-healing and recycling (i.e., reprocessing) of highly crosslinked thermosets, especially epoxy resins.^{9,10} Beside of the abovementioned “thermoplast-like thermosets,” attempts were also made to produce “thermoset-like thermoplastics” (such as polyamides with reversible crosslinks)¹¹ via DA reactions. The most explored DA reaction is that one between furan and maleimide groups.^{12–15}

Among the SMPs, polyurethanes with amorphous or crystalline polyethers or polyesters constituting the soft switch segment for shape memory performance have received considerable attention recently.¹⁶ Crosslinked PUs having excellent shape memory

Additional Supporting Information may be found in the online version of this article.

© 2016 Wiley Periodicals, Inc.

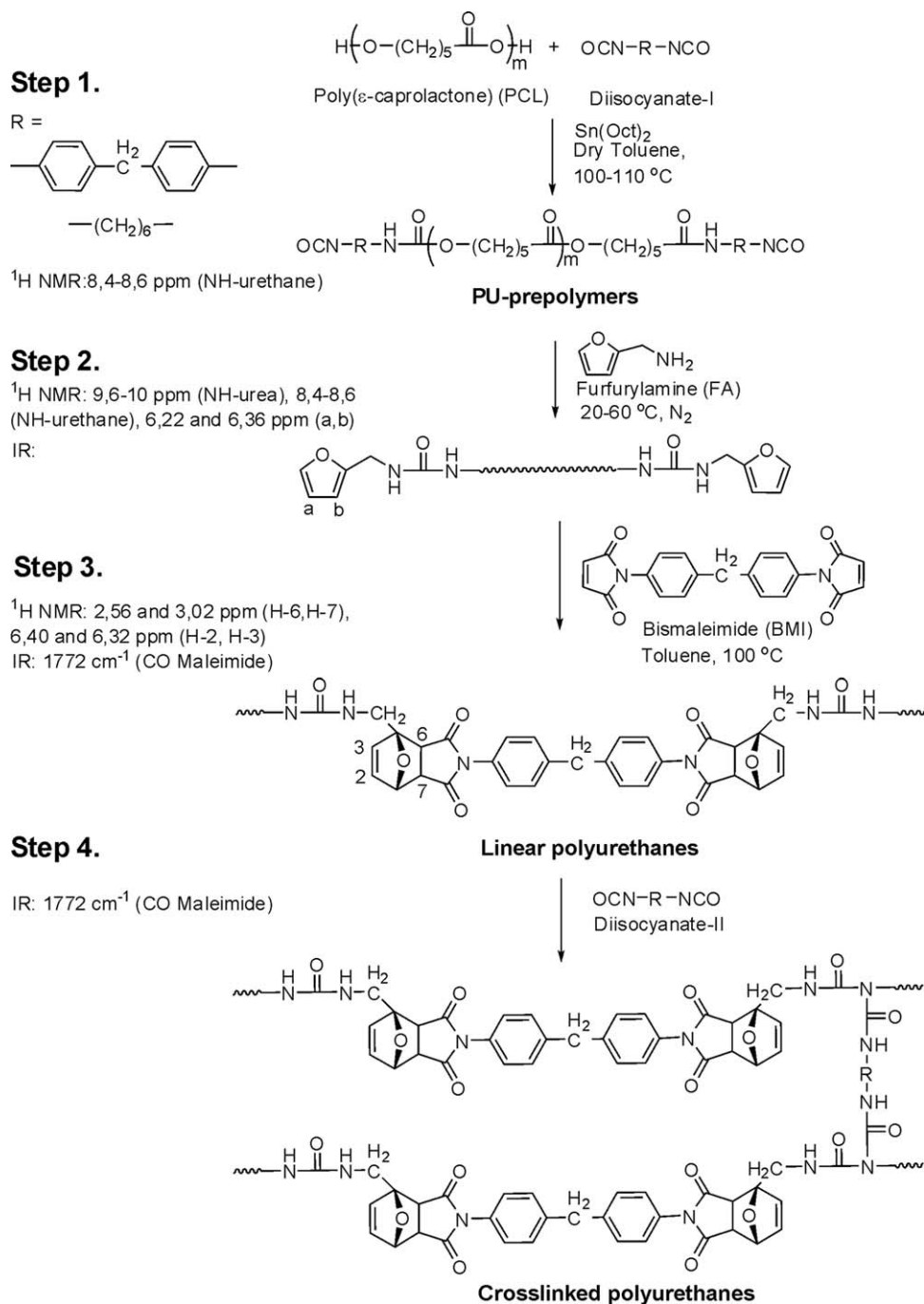


Figure 1. Synthetic route for the preparation of crosslinked polyurethanes containing DA-adducts.

properties frequently contain permanent chemical bonds as net-points. Recently, various PUs containing reversible DA bonds at the netpoints have been synthesized and shown to have shape memory¹⁷ and self-healing properties.¹⁸

Scarce reports are available on the preparation of PUs with both reversible chemical bonds in the main chain and with irreversible chemical bonds at their netpoints.¹⁹ In this article, we report the synthesis and characterization of thermoresponsive PUs containing reversible DA adducts and irreversible allophanate crosslinks. Poly(ϵ -caprolactone) (PCL) with varying

molecular weights has been selected as a crystallizable switch segment. The effects of the composition of the reaction mixture on the mechanical, thermomechanical and shape-memory properties of these PUs are discussed.

EXPERIMENTAL

Materials

Poly(ϵ -caprolactone) (PCL) ($M_n = 10$ kg/mol) from Sigma-Aldrich Chemical Co. (Darmstadt, Germany), PCL ($M_n = 25$ kg/mol) (CAPA[®] 6250), and PCL ($M_n = 50$ kg/mol) (CAPA[®]

Table I. Code, Compositions, and NCO-II Content in the Feed of Crosslinked PUs (Expressed in Molar Ratios)

| Code | Composition | Ratios in the feed | NCO-II |
|-------|------------------------|--------------------|--------|
| PU 1 | PCL(10)-MDI-FA-BMI-MDI | 1:3:2:1:1 | 0.5 |
| PU 2 | PCL(10)-MDI-FA-BMI-MDI | 1:3:2:2:1 | 0.5 |
| PU 3 | PCL(10)-MDI-FA-BMI-MDI | 1:3:2:2:2 | 1.0 |
| PU 4 | PCL(10)-MDI-FA-BMI-MDI | 1:3:2:2:3 | 1.5 |
| PU 5 | PCL(10)-MDI-FA-BMI-HDI | 1:3:2:2:1 | 0.5 |
| PU 6 | PCL(10)-HDI-FA-BMI-HDI | 1:3:2:2:1 | 0.5 |
| PU 7 | PCL(25)-MDI-FA-BMI-MDI | 1:3:2:2:1 | 0.5 |
| PU 8 | PCL(25)-MDI-FA-BMI-HDI | 1:3:2:2:1 | 0.5 |
| PU 9 | PCL(25)-HDI-FA-BMI-HDI | 1:3:2:2:1 | 0.5 |
| PU 10 | PCL(50)-MDI-FA-BMI-MDI | 1:3:2:2:1 | 0.5 |
| PU 11 | PCL(50)-MDI-FA-BMI-HDI | 1:3:2:2:1 | 0.5 |
| PU 12 | PCL(50)-HDI-FA-BMI-HDI | 1:3:2:2:1 | 0.5 |

6500) from Perstorp Holding AB (Malmö, Sweden) were used as diol components. 4,4'-methylene diphenyl diisocyanate (MDI), 1,6-hexamethylene diisocyanate (HDI), furfurylamine (FA), and 1,1'-(methylene di-4,1-phenylene)bismaleimide (BMI) were all of reagents grades and purchased from Sigma-Aldrich. Tin(II) ethylhexanoate, used as catalyst, was procured from Sigma-Aldrich. Toluene from Lab-Scan Analytical Sciences (Gliwice, Poland) was distilled over P_2O_5 and stored on sodium wire until use.

Measurements

Density of the crosslinked PUs was determined by pycnometry using distilled water as immersion liquid.

For the determinations of the degree of swelling, gel content and crosslink density, samples (dimension: $10 \times 10 \times \sim 0.3$ mm) were swollen in toluene (10 mL) at 22 °C (295 K) in a closed bottle for 24 h according to the procedure described in our earlier publication.²⁰ The degree of swelling (Q) and the gel content (G) were calculated by eqs. (1) and (2).^{20,21}

$$Q = 1 + \frac{\rho_s}{\rho_p} \left(\frac{m_2}{m_3} - 1 \right) \quad (1)$$

and

$$G(\%) = \frac{m_3}{m_1} \cdot 100 \quad (2)$$

where ρ_s and ρ_p are the densities of the solvent (toluene, ρ : 0.8669 g/cm³) and the PU polymer, respectively.

The volume fraction of the polymer in the swollen state (v_1) was determined by eq. (3):

$$v_1 = \frac{V_p}{V_s + V_p} \quad (3)$$

where V_p and V_s are the actual volumes of PU and solvent, respectively.

The crosslink density (v_e) was calculated based on the swelling results using the Flory-Rehner eq. (4)²²:

$$v_e = \frac{-[\ln(1-v_1) + v_1 + \chi \cdot v_1^2]}{V_{ms} \cdot (v_1^{1/3} - \frac{v_1}{2})} \quad (4)$$

where V_{ms} is the molar volume of the solvent.

The interaction parameter, χ between toluene and the polymer was determined by eq. (5):

$$\chi = \frac{(\delta_2 - \delta_1)^2 \cdot V_{ms}}{R \cdot T} \quad (5)$$

δ_1 and δ_2 is the solubility parameter of solvent and polymer, respectively; R is the universal gas constant and T is the absolute temperature. The Hildebrand solubility parameters of toluene and PU polymers were $\delta_1 = 18.2$ and $\delta_2 = 20.5$ (MPa)^{1/2}, respectively.²³ The molar volume of toluene (V_{ms}) and interaction parameter (χ) at 295 K were calculated to be 1.06×10^{-4} m³/mol and 0.228, respectively.

ATR FT-IR spectra were recorded on a Perkin Elmer Instruments Spectrum One FT-IR spectrometer equipped with a Universal ATR Sampling Accessory. The polymer was irradiated by IR beam through a special diamond-zinc-selenium composite prism. The average film thickness of the specimens was about 0.5 mm. Four scans were taken for each sample. The spectra were evaluated by Spectrum ES 5.0 program.

Tensile tests were carried out according to the EN ISO 527-1 standard using an Instron 4302 type tensile testing machine equipped

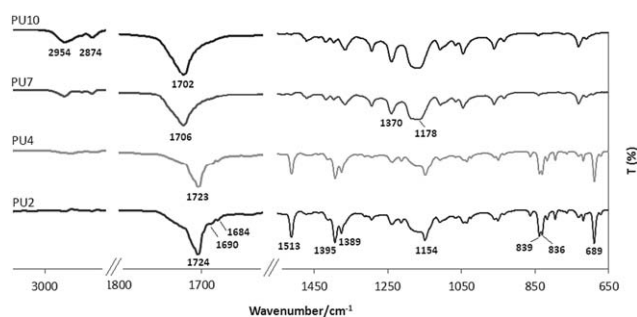


Figure 2. ATR-FTIR spectra of PUs 2, 4, 7, and 10.

Table II. Hard and Soft Segment Contents, Density, and Swelling Properties at 294 K of the Crosslinked PUs

| Code | Hard segment (wt %) | Soft segment (PCL) (wt %) | Density (g/cm ³) | Q | G (%) | v ₁ | Crosslink density (mol/cm ³) |
|-------|---------------------|---------------------------|------------------------------|------|-------|----------------|--|
| PU 1 | 13.5 | 86.5 | 1.01 | 7.8 | 89.5 | 0.189 | 2.4 × 10 ⁻⁴ |
| PU 2 | 16.1 | 83.9 | 1.14 | 9.4 | 76.7 | 0.164 | 1.8 × 10 ⁻⁴ |
| PU 3 | 17.8 | 82.2 | 1.10 | 9.6 | 75.4 | 0.171 | 2.0 × 10 ⁻⁴ |
| PU 4 | 19.4 | 80.6 | 1.14 | 6.8 | 84.8 | 0.196 | 2.6 × 10 ⁻⁴ |
| PU 5 | 15.5 | 84.5 | 1.03 | 15.1 | 54.0 | 0.215 | 1.6 × 10 ⁻³ |
| PU 6 | 14.2 | 85.8 | 1.07 | 17.2 | 44.0 | 0.204 | 2.8 × 10 ⁻⁴ |
| PU 7 | 7.1 | 92.9 | 1.04 | 39.0 | 23.2 | 0.167 | 1.9 × 10 ⁻⁴ |
| PU 8 | 6.8 | 93.2 | 1.19 | 44.8 | 37.0 | 0.075 | 4.1 × 10 ⁻⁵ |
| PU 9 | 5.9 | 94.1 | 1.17 | 26.4 | 12.5 | 0.194 | 2.6 × 10 ⁻⁴ |
| PU 10 | 3.7 | 96.3 | 1.01 | 57.0 | 35.3 | 0.078 | 4.4 × 10 ⁻⁶ |
| PU 11 | 3.5 | 96.5 | 1.02 | 64.8 | 14.7 | 0.165 | 1.8 × 10 ⁻⁴ |
| PU 12 | 3.0 | 97.0 | 1.05 | 91.0 | 15.3 | 0.108 | 8.1 × 10 ⁻⁵ |

with a 1 kN load cell. At least three dumbbell specimens were cut and tensile loaded at a crosshead speed of 50 mm/min. The thickness of the specimens varied between 0.3 and 1.1 mm.

In order to get a deeper insight into the morphology of PUs SEM pictures were taken from the fracture surface of selected specimens by Hitachi S-4800 (Hitachi High-Technologies, Tokyo, Japan) equipment. Surface of the specimens was covered with a 30 nm conductive gold layer.

The thermal properties of the synthesized PUs were examined by DSC. DSC tests were carried out in a DSC Q2000 power compensation DSC equipment (TA Instruments, New castle, DE) operating at 10 °C/min heating rate. Nitrogen flow was used as a protective atmosphere.

The weight percentage of the crystalline PCL (C_r) was calculated by eq. (6)²⁴:

$$C_r = \frac{\Delta H_m}{\chi_A \times \Delta H_m^0} \times 100 \% \quad (6)$$

where ΔH_m is the heat of fusion of the investigated PU, χ_A is the weight fraction of PCL in the corresponding PU, ΔH_m^0 is the heat of fusion of the pure 100% crystalline PCL. For the latter 135.31 J/g has been taken.²⁵

Dynamic mechanical analysis (DMA) measurements for PUs synthesized were carried out in DMA Q800 device of TA Instruments. DMA traces were monitored in tension mode (dimension of the specimens: length: 25 mm, clamped length: 12 mm, width: 7 mm, thickness: ca. 0.5 mm) at an oscillation amplitude of 0.2% using a frequency of 1 Hz and a static load of 1 N. The temperature was varied between -10 °C and 150 °C with a heating rate of 3 °C/min.

Shape memory properties were evaluated in tensile mode using the above DMA device. The specimens (clamped length × width × thickness = ca. 12 × 7 × 0.5 mm) were stretched after 10 min holding at 80 °C at a strain rate of 15 or 40%/min to 30 or 80% strain, followed by cooling quickly to 20 °C. The stress was then released and the shape fixity (R_f) determined. Shape

recovery (R_r) was measured at 0.1 N loading of the specimens (quasi free recovery) by reheating the specimens at 3 °C/min heating rate from 20 °C to 60 or 80 °C and holding there for 20 min. The shape fixity (R_f) and shape recovery ratios (R_r) are defined by eqs. (7a) and (7b):

$$R_f(\%) = \frac{l_d - l_0}{l_{80\%} - l_0} \cdot 100 \quad (7a)$$

$$R_r(\%) = \frac{l_d - l_f}{l_d - l_0} \cdot 100 \quad (7b)$$

where l_d is the sample length after removal of the tensile load during shape fixing at 20 °C, l_0 is the clamped length of the sample at 20 °C, $l_{80\%}$ is the length after stretching at 80 °C in tensile load in place, and l_f is the final recovered length of the stretched specimen.

Table III. Tensile Properties of the PUs 1-12

| Code | E (MPa) | ϵ_R (%) | σ_R (MPa) |
|-------|----------|------------------|------------------|
| PU 1 | 373 ± 11 | 872 ± 163 | 26 ± 3 |
| PU 2 | 328 ± 55 | 670 ± 36 | 23 ± 1 |
| PU 3 | 416 ± 3 | 597 ± 16 | 23 ± 0.7 |
| PU 4 | 331 ± 38 | 664 ± 269 | 18 ± 3 |
| PU 5 | 576 ± 52 | 392 ± 72 | 21 ± 1 |
| PU 6 | 380 ± 24 | 565 ± 31 | 21 ± 0.4 |
| PU 7 | 347 ± 10 | 792 ± 10 | 29 ± 1 |
| PU 8 | 353 ± 10 | 874 ± 90 | 36 ± 3 |
| PU 9 | 577 ± 32 | 304 ± 108 | 19 ± 2 |
| PU 10 | 334 ± 35 | 736.5 ± 130 | 29 ± 3 |
| PU 11 | 359 ± 67 | 795 ± 65 | 34 ± 5 |
| PU 12 | 244 ± 33 | 669 ± 29 | 25 ± 2 |

E is elastic modulus (Young's modulus), ϵ_R is the ultimate elongation, and σ_R is the stress at break.

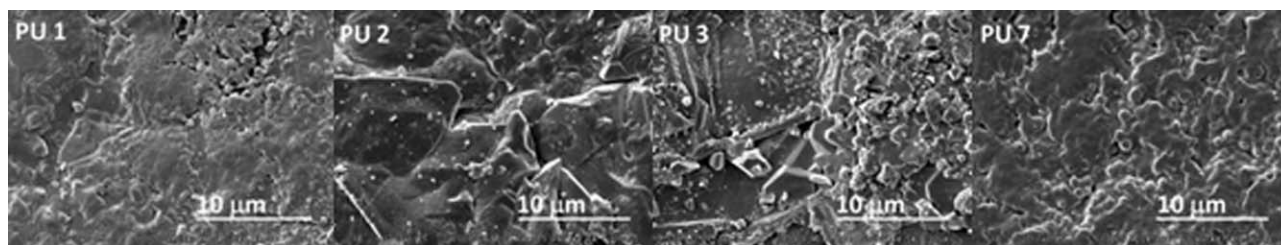


Figure 3. SEM images of PUs 1-3 and 7.

Synthesis

A typical synthetic procedure for the preparation of crosslinked PUs containing Diels-Alder adduct was as follows (see Figure 1): 5.0 g (5×10^{-4} mol, $M_n = 10$ kg/mol, 1 eq.) PCL was dissolved in dry toluene at 60 to 80 °C (50 mL; under nitrogen blanket in a 250 mL four-neck flask equipped with mechanical stirrer, dropping funnel, condenser, and nitrogen inlet). 0.375 g MDI (1.5×10^{-3} mol, MDI in 5 mL toluene, 3 equiv.) was added dropwise into the reaction mixture and reacted for 2 to 3 h at 100 to 110 °C to obtain the prepolymer. Tin(II) ethylhexanoate (2 mol %, reagent grade) was used as catalyst. To obtain linear polymer chains containing Diels-Alder adducts furfurylamine (FA, 2 eq.) was added to the isocyanate ended pre-polymer solution in one portion at 20 °C and the mixture heated to 60 to 80 °C and kept there for 0.5 h. Afterwards bismaleimide (BMI, 1 or 2 eq.) was added at the same temperature and then the reaction mixture heated to 100 to 110 °C and stirred there for 2 h. Crosslinking was achieved by introducing an additional equivalent of MDI, and the reaction stirred for further 1 h at 100 to 110 °C. The dissolved final product was poured onto Teflon® plates and dried in air. The crosslinked PUs obtained were yellow elastic films.

RESULTS AND DISCUSSION

Syntheses of Crosslinked PUs

Our aim was to synthesize crosslinked PUs containing thermoreversible DA adducts and PCL acting as a “switching” elements for shape memory performance. The synthetic route for the preparation of crosslinked PUs containing DA adducts is summarized in Figure 1.

According to Figure 1, PCLs of varying molecular weights were reacted with diisocyanate (MDI or HDI, denoted as diisocyanate-I) to yield isocyanate-ended prepolymers (Step 1). In this reaction step an excess of diisocyanate to PCL were used (OH/NCO ratios 1:3).²⁰ In step 2 the isocyanate-terminated prepolymer was further reacted with furfurylamine (FA). DA reaction was triggered between the furan of the modified prepolymer and maleimide groups of the BMI added (step 3). This resulted in linear PUs containing DA adducts. (The reversibility of the DA reaction between *N*-methoxycarbonylated furfurylamine and BMI as model compounds in deuterated dimethyl sulfoxide was supported by ¹H-NMR spectroscopy at different temperatures and the corresponding ¹H-NMR spectra are shown in the Supporting Information as Figure S1).

The crosslinking between the linear polymer chains formed in step 3 was achieved using additional amount of diisocyanate

(MDI or HDI, denoted as diisocyanate-II) to yield crosslinked PUs (step 4). The compositions of the feeds applied for the preparation of PUs 1-12 are listed in Table I (codes: PUs 1–12).

Characterization of Crosslinked PUs by IR Spectroscopy

Figure 2 shows the representative FT-IR spectra for PUs 2, 4, 7, and 10.

As seen in Figure 2, the absorption bands at 2874, 2954 cm^{-1} and at 1370, 1395 cm^{-1} are associated with the symmetric and asymmetric CH_2 stretching and bending vibrations of PCL, respectively. The absence of absorption at around 2230 cm^{-1} , characteristic for the NCO group, indicates the complete transformation of the NCO end groups. The free C=O band of PUs 2 to 6 are visible at 1702 to 1706 cm^{-1} , while in the cases of PUs 1, 7 to 12 this band appeared at 1723 to 1724 cm^{-1} . The band at 1772 cm^{-1} (C=O of maleimide part) indicates the presence of the DA adduct.^{26,27} In the FT-IR spectra of PUs the H-bonded C=O band appeared at 1684 and 1690 cm^{-1} as a shoulder of the free C=O band (1723–1724 cm^{-1}). Increasing the hard segment (i.e. diisocyanate) content and the ordered crystalline fraction of PCL may result in a shift of the corresponding C=O band to lower frequencies. In line with these observations, PUs 2 to 6 contain PCL with the lowest molecular weight ($M_n = 10$ kg/mol) and their hard segment content are thus higher (19.4–14.2%) than those of the other PU samples with higher molecular weight PCLs (3.0–7.1%). The other unusual finding is at 1513 cm^{-1} belonging to the amide II band for poly(ester-ether urethane), which occurred with much higher intensity (PUs 2–6) than for the other PU samples (PUs 1, 7–12). The band at ~ 1154 cm^{-1} with relatively high intensity

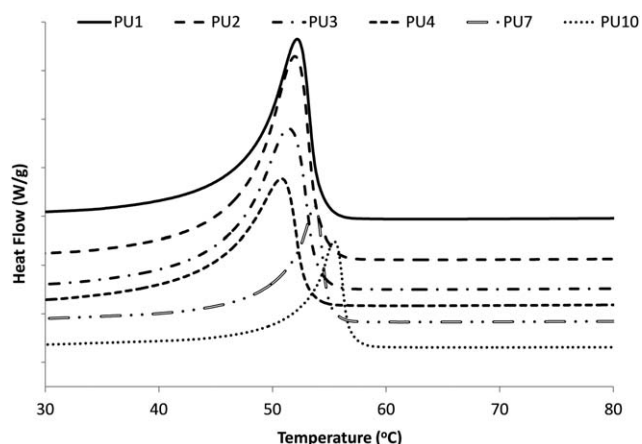


Figure 4. DSC curves (first heating) of PUs 1-4, 7, and 10.

Table IV. Melting Temperature (T_m), Melting Enthalpy (ΔH_m), and Crystallinity Values from DSC Measurements Obtained from the First Heating Cycle

| Code | PCL (M_n , kg/mol) | T_m (°C) | PCL (wt %) | ΔH_m (J/g) | Crystallinity (%) |
|-------|-----------------------|------------|------------|--------------------|-------------------|
| PU 1 | 10 | 59.6 | 86.5 | 80.8 | 68 |
| PU 2 | 10 | 59.5 | 83.9 | 63.3 | 56 |
| PU 3 | 10 | 60.0 | 82.2 | 64.2 | 58 |
| PU 4 | 10 | 59.5 | 80.6 | 58.8 | 54 |
| PU 5 | 10 | 61.9 | 84.5 | 68.9 | 60 |
| PU 6 | 10 | 49.8, 59.6 | 93.7 | 62.7 | 49 |
| PU 7 | 25 | 61.2 | 92.9 | 72.5 | 58 |
| PU 8 | 25 | 63.7 | 93.2 | 81.4 | 64.5 |
| PU 9 | 25 | 61.3 | 94.1 | 68.3 | 54 |
| PU 10 | 50 | 64.3 | 96.3 | 83.3 | 64 |
| PU 11 | 50 | 64.8 | 96.5 | 80.9 | 62 |
| PU 12 | 50 | 60.3 | 97.0 | 59.1 | 45 |

assigned to the $=C-O-C-O-C-$ vibrations appearing as a sharp peak in the FT-IR spectra of PUs 2–6.

Swelling Properties of Crosslinked PUs

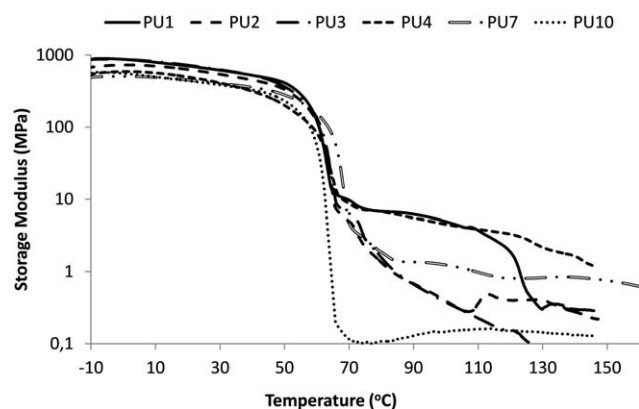
The network was characterized by results deduced from the swelling experiments. Values of the degree of swelling (Q), gel content (G), and crosslink density obtained are summarized in Table II. Gel contents of PUs 1–12 vary between 12.5% and 89.5% depending on the compositions, while the range of the

crosslink densities is in between 10^{-3} mol/cm³ and 10^{-6} mol/cm³. According to the data in Table II, the crosslink densities for PUs 2–4 increase in the order of PU 2 < PU 3 < PU 4, i.e., with the amount of MDI-2 content, as expected. Consequently, PU 2 has the highest, while PU 4 the lowest swelling degree (Q) in this series, consistently with the increase in the crosslink density. In addition, increasing the molecular weight of PCL, or applying HDI as a crosslinker, generally reduced the crosslink densities (cf. PU 2 vs. PU 10 and PU 7 vs. PU 8). Interestingly, the PUs crosslinked with HDI and containing the lowest molecular weight PCL exhibited higher crosslink densities as compared to the MDI crosslinked counterparts (cf. PU 2 vs. PU 5). This may be due to the difference in the molecular flexibilities of these diisocyanates.

Tensile Properties of Crosslinked PUs

The mechanical properties, determined in tensile measurements, are presented in Table III.

Based on the data of the series of PUs 2–4 in Table III increasing amount of crosslinker (diisocyanate-II) does not significantly influence the mechanical properties. Note that those PUs in which MDI was the coupling agent and HDI acted as the crosslinker (PUs 5, 8, 11) showed higher tensile strength values (21, 36, and 34 MPa, respectively) than those PUs produced using HDI both for the coupling and crosslinking (PU 6, 9, 12 exhibiting 21, 19, and 25 MPa tensile strength values, respectively). Furthermore, the molecular weight of PCL has only a minor effect on the values of E and σ_R . For example, for PUs 2, 7, and

**Figure 5.** Storage modulus as a function of temperature for PUs 1–4, 7, and 10.**Table V.** E' Values and Crosslink Densities (ν_e) Obtained from DMA Experiments for PUs 1–4, 7, and 10

| Code | E' (MPa) | ν_e (mol/cm ³) |
|-------|------------|--------------------------------|
| PU 1 | 6.04 | 6.7×10^{-4} |
| PU 2 | 0.89 | 9.8×10^{-5} |
| PU 3 | 0.90 | 9.9×10^{-5} |
| PU 4 | 6.08 | 6.7×10^{-4} |
| PU 7 | 1.38 | 1.5×10^{-4} |
| PU 10 | 0.12 | 1.3×10^{-5} |

Table VI. Shape Fixity and Shape Recovery Ratios for PUs 1, 2, and 7

| Code | Temperature (°C) | Initial strain (%) | R_f (%) | R_r (%) |
|------|------------------|--------------------|-----------|-----------|
| PU 1 | 80 | 80 | 99 | 36 |
| PU 2 | 80 | 80 | 99 | 43 |
| PU 2 | 60 | 30 | 99 | 57 |
| PU 7 | 80 | 80 | 100 | 80 |

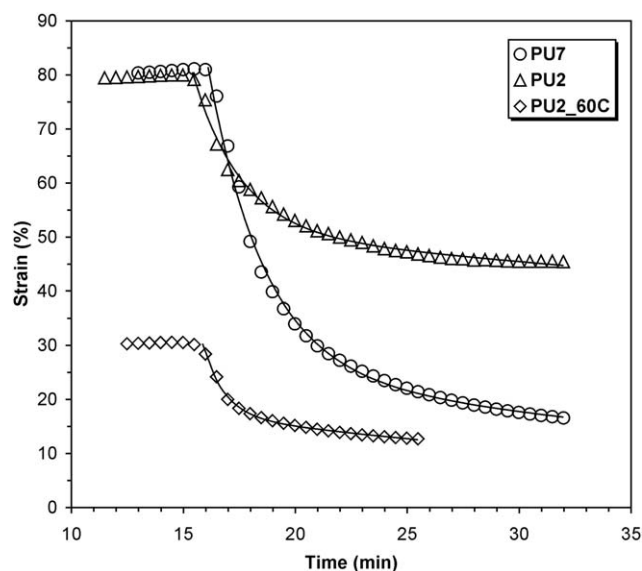


Figure 6. Strain versus time recovery curves for the samples PU 2 and PU 7 at 80°C with an initial strain of 80% and for PU 2 at 60°C with an initial strain of 30% (PU2_60C). The solid lines represent the fitted curves using eq. (9). The estimated parameter for PU 2 are: $A_1 = 28.6\%$, $A_2 = 50.8\%$, $\tau_1 = 2.1$ min, $\tau_2 = 130$ min and for PU 7: $A_1 = 58.7\%$, $A_2 = 25.6\%$, $\tau_1 = 2.5$ min, $\tau_2 = 25.6$ min, and for PU2_60C: $A_1 = 11.7\%$, $A_2 = 16.9\%$, $\tau_1 = 1.0$ min, $\tau_2 = 31.6$ min.

10, containing PCLs of $M_n = 10, 25$ and 50 kg/mol, respectively, similar values were obtained (cf. Table III).

Morphology of Crosslinked PUs

SEM investigations were also performed to learn more about the morphology of the PUs synthesized (see in Figure 3).

The fracture surfaces of PUs 1, 2, 3, and 7 reveal complex structures which implicitly indicate differences in the chemical and physical networks. As seen in Figure 3, a significant difference can be observed between SEM images of PU 2 and PU 7, where the latter one shows a more interweaving structure. This may hint for higher ductility and improved mechanical properties of PU 7 compared to PU2 which is in good agreement with the tensile test results (cf. Table III).

Thermal Behaviors of Crosslinked PUs

Note that in the PUs synthesized the PCL segment acts as “switch” via its melting/crystallization. In this respect, it is important to investigate how the allophanate network and DA adducts (formed between furan and maleimide units) influence the crystallization of PCL segment. Therefore, PUs 1-12 were investigated by DSC (see Figure 4 and Table IV).

As seen in Figure 4 the melting peaks of PCL segments were clearly detected in DSC measurements. No thermal effects associated with the presence of the DA adduct appeared in the DSC curves even at higher temperatures, most probably due to the low concentration of DA adducts. Furthermore, as shown by the data of Table IV, the highest melting temperature of PCL was found for PUs 5, 8, and 11, which were synthesized using MDI as the coupling units and HDI as the crosslinker. In PUs 2, 7, and 10, in which MDI served as for both the coupling and the crosslinking agent, the melting temperature and crystallinity values increased with increasing molecular weight of PCL. Note that for the series of PUs produced by using MDI/HDI combinations for coupling/crosslinking (PUs 5, 8, 11), the melting temperature also increased with increasing molecular weight of PCL. PUs 6, 9 and 12, where HDI worked for both coupling and crosslinking, exhibited low crystallinities. In PU 6 two different crystalline fractions were present according to two melting peaks with different temperatures (cf. Table IV).

Shape Memory Properties of Crosslinked PUs

Thermal properties, which determine the shape memory properties of PUs, were studied using dynamic mechanical analysis (DMA) in tensile mode. Storage modulus (E') as a function of temperature for PUs 1-4, 7, and 10 are shown in Figure 5. The storage modulus decreases sharply at $\approx 60^\circ\text{C}$ for all PU samples due to the melting of the crystalline PCL phase at this temperature. The DMA traces show the presence of a rubber-like plateau above T_m of the PCL in the temperature range of 70 to 120°C . The appearance of rubber-like plateau in the case of these PUs can be attributed to the interplay between physical (phase separation and related structural “mingling”) and chemical crosslinks (allophanate network). The presence of relatively long rubber-like plateau, which strongly depends on the composition (cf. Figure 5), suggests an excellent tool for shape memory programming. It is also evident that PU 7 displays two rubber-like plateaus appearing at temperature ranges of 90 to 110°C and 120 to 140°C . The first plateau is due to the presence of crosslinks (physical and chemical), while the occurrence of the second plateau at higher temperature may be the consequence of the cleavage of DA adducts, i.e., occurrence of the retro Diels-Alder (rDA) reactions. However, the remaining allophanate network, which will otherwise decomposes at higher temperature, still provide enough crosslinks to fix the polymer chains within the temperature range of 120 to 140°C . It should be born in mind that the presence of DA adducts and their decomposition at 100 to 110°C may provide an additional switch for shape memory provided that the DA reaction can be restored before the crystallization of the PCL segment. This would allow us to use such PUs as triple shape memory



Figure 7. Illustration of the shape memory behavior for PU 7: (a) permanent, (b) temporary, (c) recovered shape. [Color figure can be viewed in the online issue, which is available at wileyonlinelibrary.com.]

polymers. Considering values of the storage modulus at the rubber-like plateau region the apparent crosslink density can be calculated based on the rubber elasticity theory according to eq. (8).^{28,29}

$$v_e = \frac{E'}{3RT} \quad (8)$$

where E' is the storage modulus value at the rubbery plateau, T is the absolute temperature where the plateau modulus was read. The E' values were read at 90 °C and the related apparent crosslink density values are presented in Table V for PUs 1–4, 7, and 10.

The trend of data presented in Table V is consistent with that obtained from the swelling experiments (cf. Table II). Accordingly, the highest crosslink densities were obtained for PU 1 and PU 4 (6.7×10^{-4} mol/cm³). Furthermore, based on the data of Table V, it can also be concluded that PU 10 has the lowest E' value and crosslink density similarly to the result obtained from the swelling experiments (see Table II).

For PU 1 and PU 7 with well-defined rubbery plateau and for PU 2 having a less well-defined DMA rubbery plateau shape memory experiments were performed. In the case of PU 2 the shaping temperature and strain were also varied. The results from the shape memory tests, i.e., shape fixity (R_f) and shape recovery ratios (R_r), are given in Table VI.

As the shape memory experiments indicate, the shape fixity ratios are ~100% for all samples, most probably due to the large difference in the values of the “glassy” and the “rubbery” modulus, thus making possible excellent shape fixity.³⁰ Moderate shape recovery ratios were obtained for PU 1 and PU 2, while relatively good R_f value was determined for PU 7. Although PU 2 has a well-developed rubbery plateau, the low R_f value is most likely due to the relatively large “rubbery” modulus as compared to the “glassy” one, thus allowing slow relaxation back to the initial shape. Furthermore, PU 2 has similar R_f value to that of PU 1 in spite of the fact that the latter has no well-developed rubber-like plateau. Decreasing the extent of deformation and the deformation temperature a slight increase in the R_r value can be observed for PU 2 (Table VI).

Modeling of shape memory properties plays an important role in designing SMPs for various applications. Thus, numerous modeling approaches have been explored to describe the thermomechanical properties of SMPs.^{31–34} From this purpose, the recovery processes for PUs were analyzed in order to establish a relationship between the strains and recovery times.

Accordingly, it was found that the strain versus time curves can be well approximated using a two-exponential decay function as shown by eq. (9).

$$\varepsilon(t) = A_1 e^{-\frac{(t-t_0)}{\tau_1}} + A_2 e^{-\frac{(t-t_0)}{\tau_2}} \quad (t \geq t_0) \quad (9)$$

where ε is the strain, A_1 and A_2 are the pre-exponential factors, τ_1 and τ_2 denote the relaxation times, and t_0 is the time at which the strain starts to decrease.

As seen in Figure 6 the curves fitted by eq. (9) match the experimental strain versus time data very well. The fast relaxation

mode (τ_1), which is in the range of 1 to 3 min, can be rendered to the strain release induced by the relatively rapid melting of the crystalline PCL phase, while the τ_2 mode, being in the range of 25 to 130 min, can be associated with a slower relaxation process necessary for the polymer chains to regain their original conformations.

For the visual illustration of the shape memory behavior, a thin strip from PU 7 was cut and deformed at 70 °C (i.e., above the melting temperature of PCL segment) in water bath and then cooled it to room temperature to set the temporary shape (Figure 7). Its re-immersion into the warm water bath resulted in the expected shape recovery.

CONCLUSIONS

Crosslinked shape memory polyurethanes containing reversible DA adducts were synthesized. The soft segments working as the switching segment for shape memory performance were poly(ϵ -caprolactone) (PCL) with varying molecular weights ($M_n = 10$ kg/mol, 25 kg/mol, 50 kg/mol), while the hard segments were composed of diisocyanates (4,4'-methylene diphenyl diisocyanate (MDI), 1,6-hexamethylene diisocyanate (HDI)), furfurylamine (FA), and bismaleimide (BMI). The synthetic strategy for the preparation of these PUs included the reaction of PCL with MDI or HDI to obtain isocyanate-ended prepolymers followed by their reaction with FA, then with BMI that resulted in the formation of linear PUs containing DA adducts. The crosslinking between the linear chains was achieved using an excess of MDI or HDI. The presence of the DA adduct in the PUs synthesized was supported by infrared spectroscopy, while the crosslinked structure was proved by swelling experiments and dynamic mechanical analysis (DMA).

According to the results of DMA, above T_m of the PCL a well-developed rubber-like plateau was obtained indicating the presence of an efficient network. The plateau range allowed us to set different programming for shape memory function that was demonstrated on some samples. Furthermore, it was also suggested that DA adducts in the network provide an additional switch via rDA reactions that may allow further programming for triple shape function. It was also shown that the shape recovery process of PUs in time can be well described by a two phase exponential decay.

The novel PUs may find their applications among the T_m -based shape memory polymers and due to the presence of reversible chemical bonds in the network, self-healing PUs assisted by shape memory properties can also be developed.

ACKNOWLEDGMENTS

The work reported here was supported by the TÁMOP-4.2.2.A-11/1/KONV-2012-0036 project co-financed by the European Union (EU) and the European Social Fund, and OTKA SNN 114547.

REFERENCES

- Hager, M. D.; Bode, S.; Weber, C.; Schubert, U. S. *Prog. Polym. Sci.* **2015**, *49*, 3.

2. Harper, M.; Guoqiang, L. *Polymer* **2013**, *54*, 2199.
3. Berg, G. J.; McBride, M. K.; Wang, C.; Bowman, C. N. *Polymer* **2014**, *55*, 5849.
4. Karger-Kocsis, J.; Kéki, S. *Expr. Polym. Lett.* **2014**, *8*, 397.
5. Maeda, T.; Otsuka, H.; Takahara, A. *Prog. Polym. Sci.* **2009**, *34*, 581.
6. Lewis, L. C.; Dell, M. E. *J. Polym. Sci. Part B: Polym. Phys.* **2016**, *54*, 1865.
7. Zhong, Y.; Wang, X.; Zheng, Z.; Du, P. *J. Appl. Polym. Sci.* **2015**, *132*, DOI: 10.1002/app.41944.
8. Chen, X.; Dam, M. A.; Ono, K.; Mal, A.; Shen, H.; Nutt, S. R.; Sheran, K.; Wudl, F. *Science* **2002**, *295*, 1698.
9. Liu, Y. L.; Chuo, T. W. *Polym. Chem.* **2013**, *4*, 2194.
10. Kuang, X.; Liu, G.; Dong, X.; Liu, X.; Xu, J.; Wang, D. *J. Polym. Sci. Part A: Polym. Chem.* **2015**, *53*, 2094.
11. Djidi, D.; Mignard, N.; Taha, M. *Ind. Crops. Prod.* **2015**, *72*, 220.
12. Gandini, A. *Prog. Polym. Sci.* **2013**, *38*, 1.
13. Jaudouin, O.; Robin, J. J.; Lopez-Cuesta, J. M.; Perrin, D.; Imbert, C. *Polym. Int.* **2012**, *61*, 495.
14. Zhang, L.; Brostowitz, N. R.; Cavicchi, K. A.; Weiss, R. A. *Macromol. React. Eng.* **2014**, *8*, 81.
15. Rivero, G.; Nguyen, L. T.; Hillewaere, X. K. D.; Du, Prez, F. E. *Macromolecules* **2014**, *47*, 2010.
16. Azra, C.; Ding, Y.; Plummer, C. J. G.; Manson, J. A. E. *Eur. Polym. J.* **2013**, *49*, 184.
17. Gaina, C.; Ursache, O.; Gaina, V.; Varganici, C. D. *Expr. Polym. Lett.* **2013**, *7*, 636.
18. Yoshie, N.; Saito, S.; Oya, N. *Polymer* **2011**, *52*, 6074.
19. Heo, Y.; Sodano, H. A. *Adv. Funct. Mater.* **2014**, *24*, 5261.
20. Czifrák, K.; Karger-Kocsis, J.; Daróczy, L.; Zsuga, M.; Kéki, S. *Macromol. Chem. Phys.* **2014**, *215*, 1897.
21. Kelch, S.; Steuer, S.; Schmidt, M. A.; Lendlein, A. *Biomacromolecules* **2007**, *8*, 1018.
22. Sekkar, V.; Gopalakrishnan, S.; Devi, A. K. *Eur. Polym. J.* **2003**, *39*, 1281.
23. Castro, M.; Lu, J.; Bruzard, S.; Kunar, B.; Feller, J. F. *Carbon* **2009**, *47*, 1930.
24. Jiang, S.; Ji, X.; An, L.; Jiang, B. *Polymer* **2001**, *42*, 3901.
25. Crescenzi, V.; Manzini, G.; Calzolari, B.; Borri, C. *Eur. Polym. J.* **1972**, *8*, 449.
26. Adachi, K.; Achimuthu, A. K.; Chujo, Y. *Macromolecules* **2004**, *34*, 9793.
27. Rueda-Larraz, L.; Fernandez d'Arlas, B.; Tercjak, A.; Ribes, A.; Mondragon, I.; Eceiza, A. *Eur. Polym. J.* **2009**, *4*, 2096.
28. Krongauz, V. V. *J. Therm. Anal. Calorimetry* **2010**, *102*, 435.
29. Krongauz, V. V. *Thermochim. Acta* **2010**, *503-504*, 70.
30. Ratna, D.; Karger-Kocsis, J. *J. Mater. Sci.* **2008**, *43*, 254.
31. Azra, C.; Plummer, C. J. G.; Manson, J. A. E. *Smart Mater. Struct.* **2013**, *22*, 075037.
32. Yu, K.; Ge, Q.; Qi, H. *J. Nat. Commun.* **2014**, *5*, 3066.
33. Chen, J.; Liu, L.; Liu, Y.; Leng, J. *Smart Mater. Struct.* **2014**, *23*, 055025.
34. Kuki, Á.; Czifrák, K.; Karger-Kocsis, J.; Zsuga, M.; Kéki, S. *Mech. Time-Depend. Mater.* **2015**, *19*, 87.